

## Microstructure and Electrochemical Distinctiveness of $\beta$ -Nickel Hydroxide by means of Zinc Additive and pH

C.R. RAVI KUMAR<sup>1,2</sup>, P. KOTTEESWARAN<sup>3</sup>, V. BHEEMA RAJU<sup>4</sup>, B. SHRUTHI<sup>4</sup>,  
M.S. SANTOSH<sup>5,\*</sup>, H.P. NAGASWARUPA<sup>1</sup>, M.S. SHIVKUMAR<sup>6</sup> and A. MURUGAN<sup>2</sup>

<sup>1</sup>Research Centre, Department of Chemistry, East West Institute of Technology, Bangalore-560 091, India

<sup>2</sup>Department of Chemistry, Kalasalingam University, Anandnagar, Srivilliputtur-626126, Tamilnadu, India

<sup>3</sup>Department of Chemistry, Renganayagi Varatharaj College of Engineering, Salvarpatti-626 128, India

<sup>4</sup>Department of Chemistry, Dr. Ambedkar Institute of Technology, Bangalore-560 056, India

<sup>5</sup>Centre for Emerging Technologies, Jain University, Jain Global Campus, 45th km, NH-209, Jakkasandra Post, Kanakapura Taluk, Ramanagaram-562 112, India

<sup>6</sup>Department of Chemistry, ACS College of Engineering, Bangalore-560 074, India

\*Corresponding author: E-mail: santoshgulwadi@gmail.com

Received: 15 June 2015;

Accepted: 7 August 2015;

Published online: 5 December 2015;

AJC-17654

The properties of zinc additive and precipitation pH values on the electrochemical and microstructural characteristics of  $\beta$ -nickel hydroxide materials prepared by co-precipitation method have been studied. All the prepared nickel hydroxide samples showed an irregular flakes shape. A correlation between structural characteristics and electrochemical activity of  $\beta$ -nickel hydroxide has been established. The degree of crystallinity, crystallite size and crystal inter sheet distance of  $\beta$ -Ni(OH)<sub>2</sub> were strongly associated with the pH values of the co-precipitation reaction. The electrochemical activity is represented by the (101) diffraction line, which increases with rising pH and the percentage of zinc additive. The percentage of SO<sub>4</sub><sup>2-</sup>, CO<sub>3</sub><sup>2-</sup> and H<sub>2</sub>O molecules adsorbed by  $\beta$ -Ni(OH)<sub>2</sub> crystals and the thermal stability of  $\beta$ -Ni(OH)<sub>2</sub> were related to pH. In moderately elevated pH values, the prepared  $\beta$ -Ni(OH)<sub>2</sub> materials possessed a condensed crystallite size and the substandard thermal stability. All these characteristics were expected to obtain better electrochemical activity from  $\beta$ -nickel hydroxide in nickel based secondary batteries.

**Keywords:**  $\beta$ -Nickel hydroxide, pH, Zinc additive, Co-precipitation reaction, Diffraction lines,  $d_{101}$ .

### INTRODUCTION

$\beta$ -Nickel hydroxide is an active material in rechargeable alkaline nickel based batteries as cathode (e.g. Ni/Fe, Ni/Zn, Ni/Cd, Ni/H<sub>2</sub> and Ni/MH). The practical magnitude of the structure of  $\beta$ -nickel hydroxide and its electrochemical properties are not only restricted to battery applications, but also find applications in fuel cells, electrochemical capacitors etc. Nickel hydroxide exists in two polymorphic forms,  $\alpha$ - and  $\beta$ -Ni(OH)<sub>2</sub>, on charging (oxidation)  $\alpha$ -Ni(OH)<sub>2</sub> transforms to  $\gamma$ -NiOOH and  $\beta$ -Ni(OH)<sub>2</sub> transforms to  $\beta$ -NiOOH, respectively [1,2]. These are structurally modified but their degree of hydration is different. Among these different polymorphic nickel hydroxide materials, the  $\beta$ -form is widely used as the cathode material in nickel based secondary batteries [3].  $\beta$ -Ni(OH)<sub>2</sub> structure arises through a hexagonal brucite shape of an inter-sheet distance of  $c_0 = 4.60 \text{ \AA}$  and a Ni-Ni atom distance of  $\alpha_0 = 3.12 \text{ \AA}$ . In a strong alkaline electrolyte,  $\beta$ -Ni(OH)<sub>2</sub> is stable

and frequently favours a reversible material for the production of nickel electrode.  $\beta$ -Ni(OH)<sub>2</sub> is a good active material for reversibility when charged to  $\beta$ -NiOOH, which has a similar layered structure with lattice parameters  $c_0 = 4.8 \text{ \AA}$  and  $\alpha_0 = 2.82 \text{ \AA}$ . On extended charging, however,  $\beta$ -NiOOH is converted to  $\gamma$ -NiOOH, whose  $c_0$  is  $7.0 \text{ \AA}$ , that is created due to overcharging, charging rate or the due to high concentration of the electrolyte [4]. The exchange of  $\beta$ -NiOOH phase to  $\gamma$ -NiOOH phase is a result of great volumetric modification and this results in enlargement of the thickness of nickel electrode and separates the formation of aeration from electrolyte. The formation of  $\gamma$ -NiOOH significantly damages the nickel electrode which results in failure of the battery. Some additives like Zn, Co and Cd have been used as additives to reduce the formation of the amount of  $\gamma$ -NiOOH in the preparation of  $\beta$ -Ni(OH)<sub>2</sub> material [5]. Compared to Co and Cd that have low rates of reactivity, zinc-ion had better performance [6]. In addition, the fact that Co is significantly expensive and Cd is

poisonous to the surroundings makes them unsuitable to be used in batteries. The  $\alpha$ -Ni(OH)<sub>2</sub>, with a nearly indistinguishable  $c_0$  parameter (8.0 Å) as compared to that of  $\gamma$ -NiOOH is formed when discharging  $\gamma$ -NiOOH phase, which is not stable in alkaline solution. The different phases of nickel hydroxide with interslab distance are shown in Fig. 1.

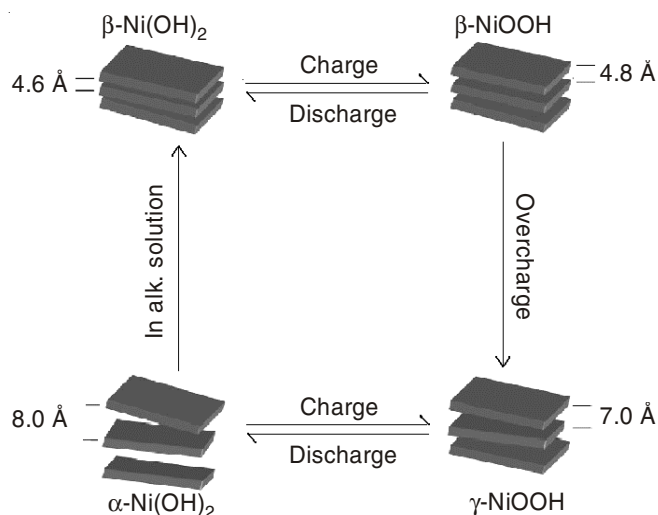


Fig. 1. Different phases of Ni(OH)<sub>2</sub> with interslab space as represented by Bode

The proton incorporation and departure from the hexagonal structure of  $\beta$ -Ni(OH)<sub>2</sub> takes place in cell reaction due to charge/discharge process without changing the crystal structure of  $\beta$ -Ni(OH)<sub>2</sub>. The magnitude of proton diffusion coefficient in  $\beta$ -Ni(OH)<sub>2</sub> enhances the electrochemical activity of  $\beta$ -Ni(OH)<sub>2</sub> material, which is strongly associated to its microstructure. The better charge/discharge cycling behaviour is obtained when  $\beta$ -Ni(OH)<sub>2</sub> material belongs to smaller crystallite size and more crystalline defects having greater chemical proton diffusion coefficient. These results will moderate the polarization of protons during charge/discharge [3,7].

The microstructural characteristics of nickel hydroxide materials prepared by co-precipitation method are closely associated to factors of the preparation route, such as reagent solutions, temperature during reaction, drying temperature, pH value, additive and additive percentage, *etc.* [8]. Out of these preparation route factors, the pH value and percentage of zinc additive are the key features that affect the crystal and chemical structural characteristics of  $\beta$ -Ni(OH)<sub>2</sub>. An effort is made through this article to provide useful information on the influence of the percentage of zinc additive and pH values on the structure and reactivity of  $\beta$ -Ni(OH)<sub>2</sub> materials. The structure and the amounts of SO<sub>4</sub><sup>2-</sup>, CO<sub>3</sub><sup>2-</sup> and H<sub>2</sub>O adsorbed in the  $\beta$ -Ni(OH)<sub>2</sub> materials are studied by using scanning electron microscope (SEM), X-ray diffraction (XRD), Fourier transform infrared (FTIR) spectroscopy, thermogravimetric (TG) and differential thermo gravimetric (DTG) analyses.

## EXPERIMENTAL

**Preparation of  $\beta$ -nickel hydroxide materials with different concentration of zinc additive:**  $\beta$ -Ni(OH)<sub>2</sub> samples with zinc additive have been prepared *via* co-precipitation method;

NiSO<sub>4</sub> and NaOH were used as reagents in their synthesis. 4 M NaOH solution was added drop wise into 100 mL of 1 M metal salt solution mixture (having appropriate ratio containing 2, 4, 6 and 8 weight % of 1 M ZnSO<sub>4</sub> with 1 M NiSO<sub>4</sub> solution). The temperature of the reactor was maintained at 50 °C. The pH of the precipitate was maintained by the addition of 4 M NaOH solution from the burette and pH value was noted using by digital pH meter using glass electrode. The excess of SO<sub>4</sub><sup>2-</sup> and OH<sup>-</sup> ions in the obtained green precipitate was removed by washing it with distilled water till the filtrate became neutral, which was checked using pH paper and the solution was filtered. The nickel hydroxide precipitate was then dried at 90 °C and ground into a fine powder using mortar. The prepared  $\beta$ -Ni(OH)<sub>2</sub> samples and their names with different pH and percentage of zinc additive were shown schematically in Fig. 2.

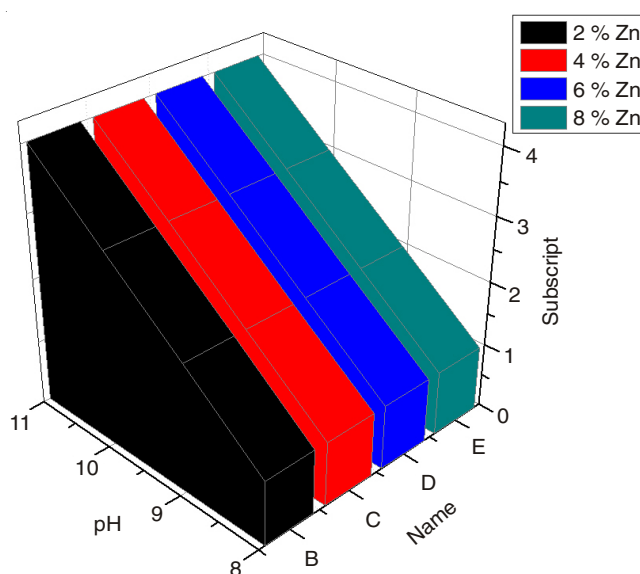


Fig. 2. Different  $\beta$ -Ni(OH)<sub>2</sub> samples names in dissimilar pH and different percentage of zinc additive

**Structural of  $\beta$ -nickel hydroxide samples:** The Philips X<sup>3</sup>pert-PRO X-ray diffractometer with graphite monochromatized CuK $\alpha$  ( $\lambda = 1.5418$  Å) radiation, at a scan rate of 10° min<sup>-1</sup> and 2 $\theta$  steps of 0.05° was used to record the characterization of XRD of prepared nickel hydroxide samples. Thermo Nicolet, Avatar 370 using DTGS detector (KBr pellets, resolution 4 cm<sup>-1</sup>) in the region 4000-400 cm<sup>-1</sup> was used for FTIR characterization. Perkin Elmer, Diamond model in the region from 0 to 750 °C which had a sensitivity of 0.2 mg was used for TG and DTG characterization.

## RESULTS AND DISCUSSION

**Surface studies:** The surface of Ni(OH)<sub>2</sub> samples with different percentage of additives was studied by scanning electron microscope (SEM). All prepared samples exhibit an irregular flakes shape shown in Fig. 3.

**Phase analysis by XRD:** The  $\beta$  phase of prepared Ni(OH)<sub>2</sub> samples were confirmed by XRD peaks at (001) ( $d_{4.60}$ ), (100) ( $d_{2.70}$ ), (101) ( $d_{2.34}$ ), (102) ( $d_{1.76}$ ), (110) ( $d_{1.56}$ ) and (111) ( $d_{1.48}$ ) are shown in Fig. 4. The crystal lattice having some disorders are differentiated by the full-width of half maximum intensity

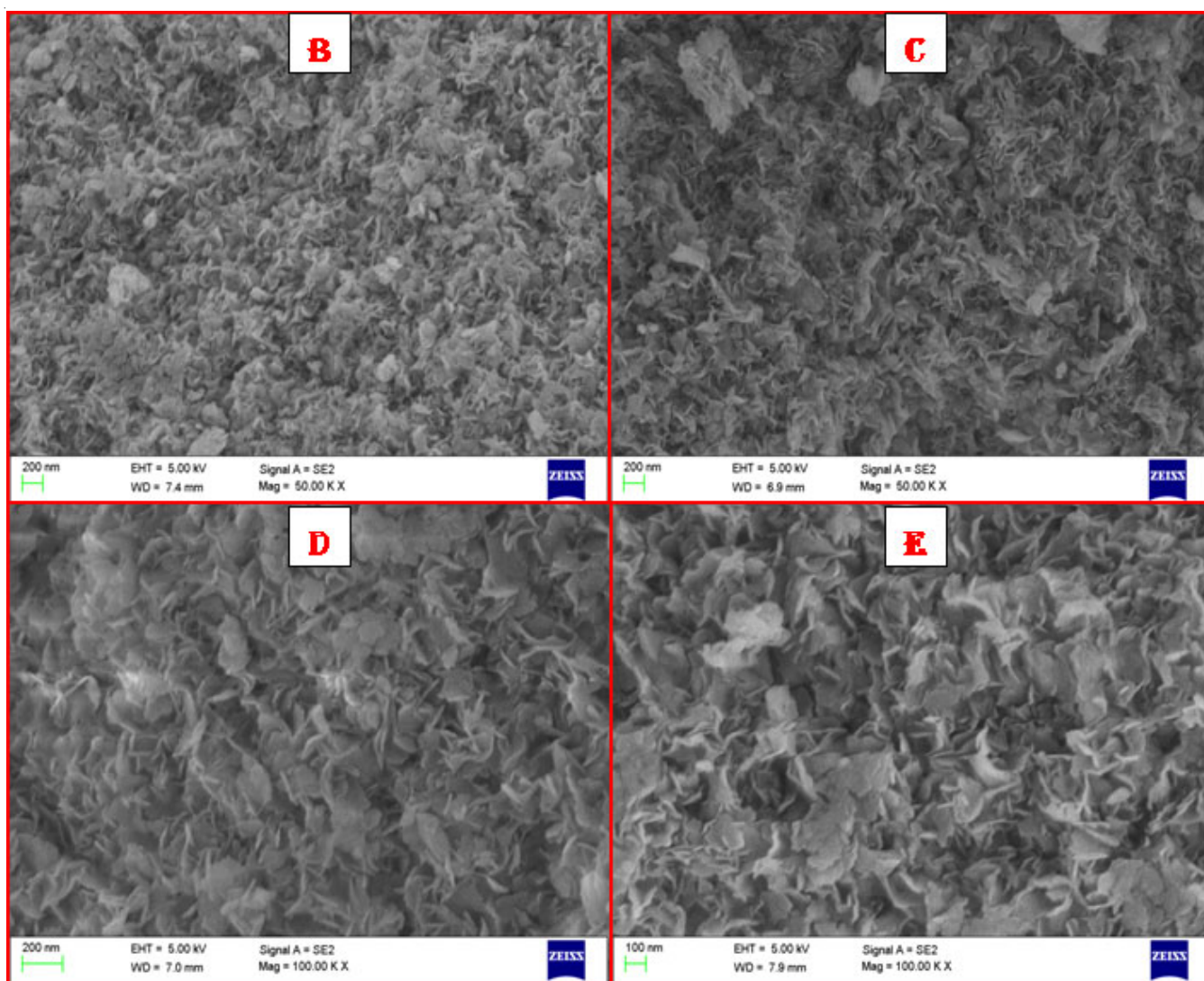


Fig. 3. SEM images of B (2 % Zn), C (2 % Zn), D (6 % Zn) and D (8 % Zn)

(FWHM) of the (001), (101) and (102) reflection lines [9,10]. The  $d_{001}$  value corresponds to interlayer distance  $c_0$  of a brucite-type in hexagonal structure of  $\beta$ -Ni(OH)<sub>2</sub>. The Ni-Ni distance within the layers of  $\beta$ -Ni(OH)<sub>2</sub> characterized by the  $d_{100}$  or  $d_{110}$  value is denoted by  $\alpha$ , where  $\alpha = (2/\sqrt{3}) d_{100}$  or  $2d_{110}$  [11].

The X-ray diffraction of samples B<sub>1</sub>, B<sub>2</sub>, C<sub>1</sub>, C<sub>2</sub>, D<sub>1</sub>, D<sub>2</sub>, E<sub>1</sub> and E<sub>2</sub> show broad peaks as compared to that of samples B<sub>3</sub>, B<sub>4</sub>, C<sub>3</sub>, C<sub>4</sub>, D<sub>3</sub>, D<sub>4</sub>, E<sub>3</sub> and E<sub>4</sub>. This indicates that the prepared samples in lower pH are poorly crystallized compared to the samples with superior pH values, having sharp reflection peaks, which indicates that the degree of ordering and crystallinity of  $\beta$ -Ni(OH)<sub>2</sub> have increased. The pH values and proportion of zinc additive in  $\beta$ -Ni(OH)<sub>2</sub> materials are directly related to crystal growth orientation. The (101) and (001) reflections are intensive in the X-ray diffraction patterns of samples B<sub>4</sub>, C<sub>4</sub>, D<sub>4</sub> and E<sub>4</sub> which shows that the crystal growth of  $\beta$ -nickel hydroxide in the direction of “c-axis” of layered structure enhances through pH and zinc additive. The electrochemical activity is represented by the (101) diffraction line, which increases with rising pH and the proportion of zinc additive (6 %). The influence of  $d_{101}$  on zinc content and pH are shown in Fig. 5.

The  $d_{001}$  diffraction line width increases with increasing pH and the gain of zinc additive because Ni<sup>2+</sup> ions with an ionic radius of 0.69 Å were substituted with Zn<sup>2+</sup> ions with a superior ionic radius of 0.74 Å and also because of the substitution of a fewer electronegative zinc metal (Zn: 1.65, Ni: 1.91) in the crystal lattice. The influence of  $d_{001}$  on zinc content and pH are shown in Fig. 6.

**FTIR spectra:** Fig. 7 shows the FTIR spectra of prepared Ni(OH)<sub>2</sub> samples B<sub>1</sub>-E<sub>4</sub>. In addition to XRD characterization the FTIR spectra are useful to investigate the structure of Ni(OH)<sub>2</sub>. It shows all prepared samples of Ni(OH)<sub>2</sub> are of  $\beta$ -type at positions: (a) 3641 cm<sup>-1</sup> due to the  $\nu$ (OH) stretching vibration which indicates that OH ions are in a free configuration; (b) 515 cm<sup>-1</sup> due to the hydroxyl groups lattice vibration  $\delta$ (OH); and (c) 460 cm<sup>-1</sup> due to the Ni-O lattice vibration  $\nu$ (Ni-O) [12,13].

All prepared samples exhibited a  $\beta$ -form which was confirmed by the presence of strong peak between 3700-3300 cm<sup>-1</sup> [14]. While for the  $\alpha$ -phases, the narrow line at 3641 cm<sup>-1</sup> signifies the presence of H-bonds. However, the  $\alpha$ -phase was represented by the presence of a very broad absorption peak around 3500 cm<sup>-1</sup> [15]. The presence of a definite amount of

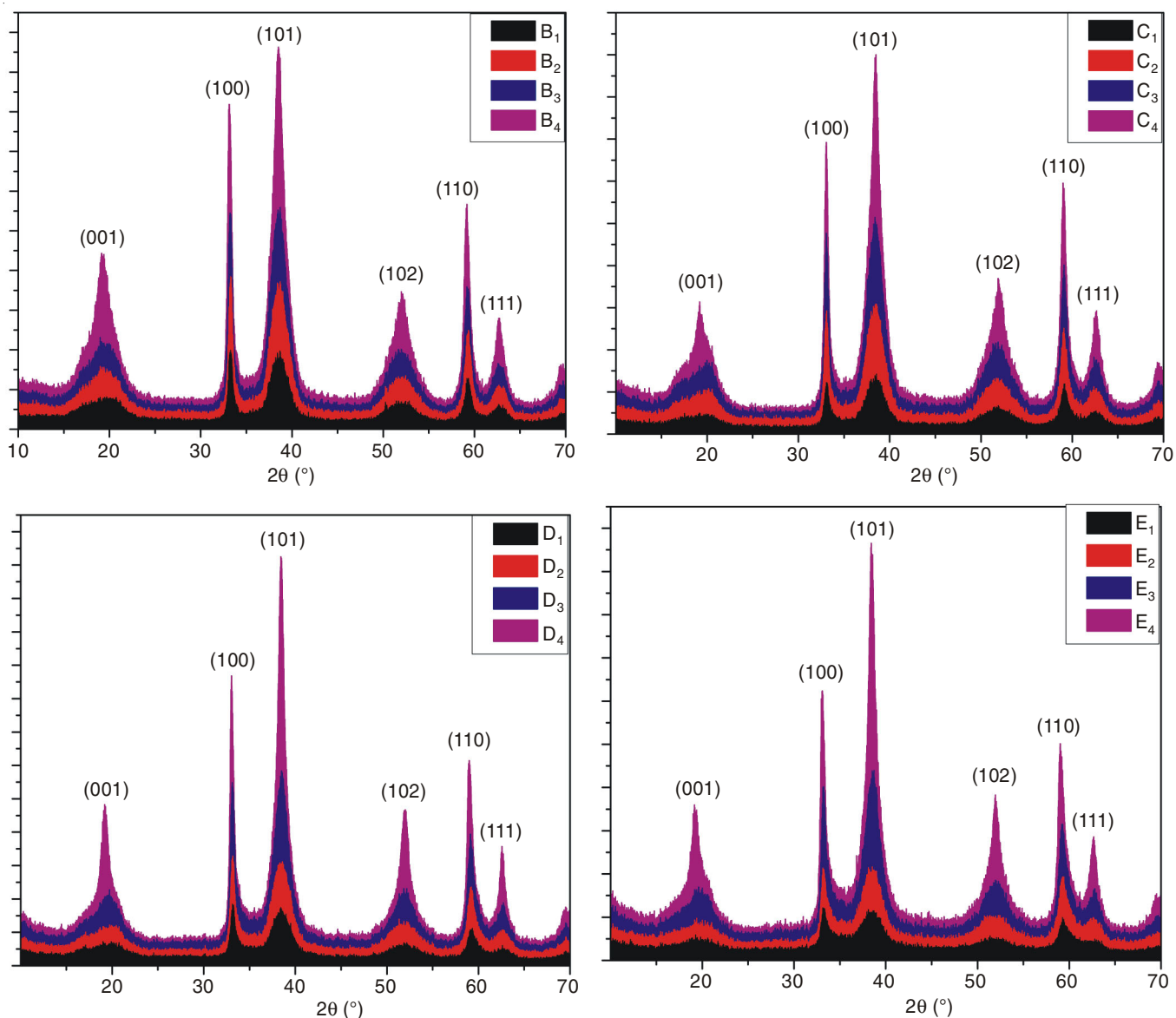


Fig. 4. XRD patterns of  $\beta$ -Ni(OH)<sub>2</sub> samples with Zinc additive (B-2 wt %, C-4 wt %, D-6 wt % and E-8 wt %) synthesized at different pH (8, 9, 10 and 11) values

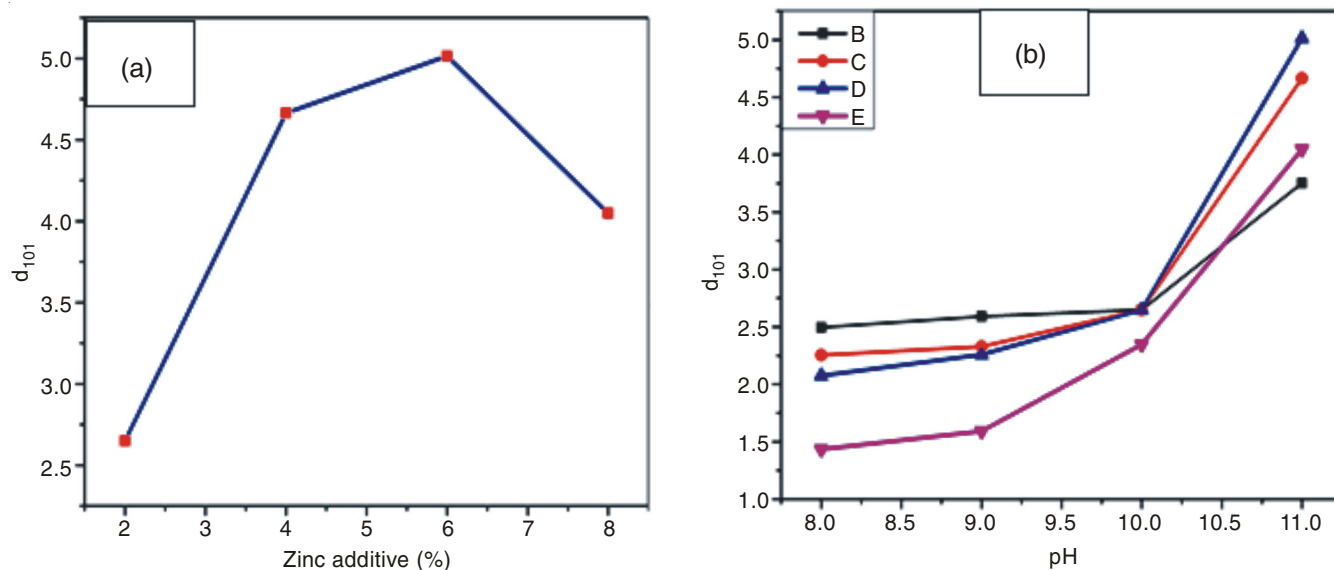


Fig. 5. Influence of (a) zinc content, B: 2 wt %; C: 4 wt %; D: 6 wt %; E: 8 wt % (b) pH on  $d_{101}$  value

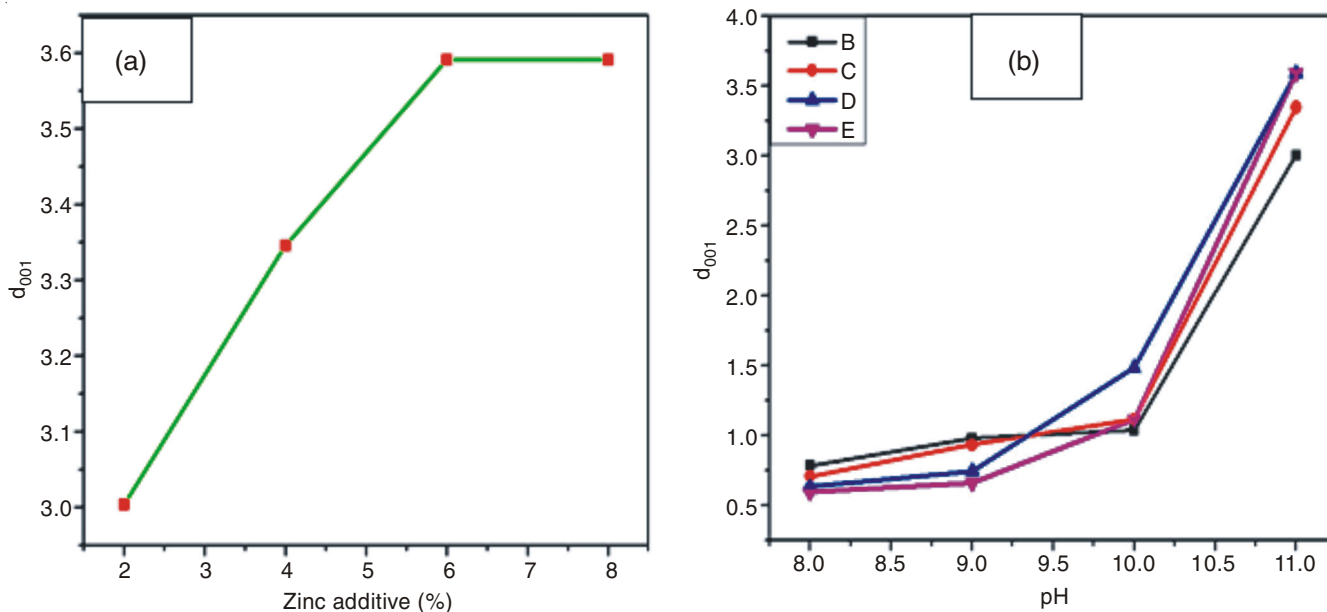


Fig. 6. Influence of (a) Zinc content, B: 2 wt %; C: 4 wt %; D: 6 wt %; E: 8 wt % (b) pH on  $d_{001}$  value

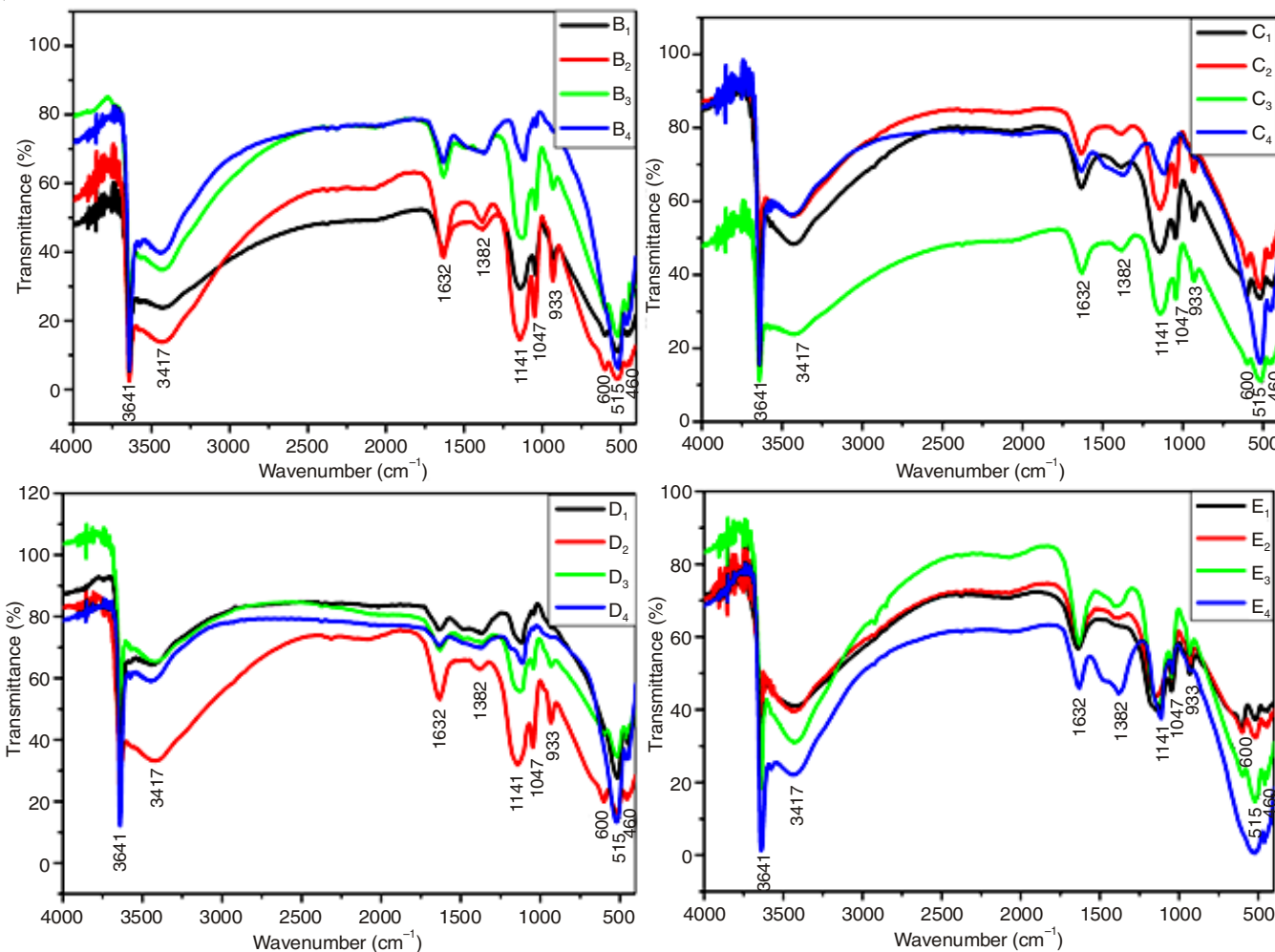


Fig. 7. IR spectra of  $\beta$ -Ni(OH)<sub>2</sub> samples with zinc additive (B-2 wt %, C-4 wt %, D-6 wt % and E-8 wt %) synthesized at dissimilar pH (8, 9, 10 and 11) values

water molecules adsorbed on the  $\beta$ -Ni(OH)<sub>2</sub> materials were confirmed by the appearance of big bands around 3417 and 1632  $\text{cm}^{-1}$  and were due to the  $\nu(\text{H}_2\text{O})$  stretching vibration

and the  $\delta(\text{H}_2\text{O})$  bending vibration of water molecules. The amount of water molecules adsorbed by  $\beta$ -Ni(OH)<sub>2</sub> samples decrease with increasing pH which was confirmed by the

decrease in the intensity of the above two bands. The same was also confirmed once again by TG and DTG studies.

The presence of carbonate and sulphate ions were observed in the range of 1400-500  $\text{cm}^{-1}$ . The bands at 1141, 933, 600  $\text{cm}^{-1}$  and the bands at 1382 and 1047  $\text{cm}^{-1}$  are characteristics of  $\text{SO}_4^{2-}$  and  $\text{CO}_3^{2-}$  ions respectively.  $\text{NiSO}_4$  was used for precipitation as it was the main source of  $\text{SO}_4^{2-}$  anions present in the prepared samples. Because of the dissolution of  $\text{CO}_2$  in air during synthesis, the peaks corresponding to  $\text{CO}_3^{2-}$  anions were visible in the prepared materials. Nickel hydroxide samples containing these anions are present in adsorbed form which is indicated by the value of interlayer distance  $c_0$  of hexagonal structure of  $\beta\text{-Ni(OH)}_2$  (4.6 Å) for permitting  $\text{SO}_4^{2-}$  anion which needed an interslab space of 9 Å [16]. The IR spectral peaks of  $\text{SO}_4^{2-}$  bands for samples prepared at low pH exhibited the largest intensity, while the  $\text{CO}_3^{2-}$  bands were missing. In addition, the intensity of  $\text{SO}_4^{2-}$  bands decreased for samples prepared at higher pH values but in case of  $\text{CO}_3^{2-}$  bands, the intensities were highly apparent and increased with increasing pH values. Further,  $\text{SO}_4^{2-}$  can be an ideal replacement for  $\text{CO}_3^{2-}$  ions that arises with an increase in pH value and with a selectivity of the anions during adsorption. The order of favourable anion adsorption in  $\beta\text{-Ni(OH)}_2$  is:  $\text{CO}_3^{2-} \gg \text{SO}_4^{2-} > \text{Cl}^- > \text{NO}_3^-$  [17].  $\beta\text{-Ni(OH)}_2$  powders prepared at a higher pH value exhibited a decrease in the sulphate ion content, while the intensity of  $\delta(\text{OH})$  lattice vibration (515  $\text{cm}^{-1}$ ) band was found to increase.

**TG and DTG analyses:** The crystal structure and the electrochemical properties of  $\beta\text{-Ni(OH)}_2$  were strongly related to the amount of adsorbed water in the prepared samples. According to the literature, the water content in  $\beta\text{-Ni(OH)}_2$  and  $\alpha\text{-Ni(OH)}_2$  phases were reported to be 0 to 0.3 molar fraction and 0.3 to 0.7 molar fraction respectively [18]. The water content and the dehydration reactions of  $\beta\text{-Ni(OH)}_2$  were examined by using TG and DTG. Two weight loss regions have been observed in the TG and DTG curves for all prepared samples, *i.e.* the first region from room temperature to 250 °C and the second region from 250 to 450 °C. These regions are clearly identified in DTG curves. Looking at the reactions involved in these two regions; the first region is due to dehydration reaction:



The second region is due to decomposition reaction,



It was confirmed that from TG and DTG curves, the adsorbed water molecules decrease with increasing pH because of a decrease in the decomposition temperature with pH.

## Conclusion

From the above studies, it was observed that the electrochemical and microstructural characteristics of  $\beta$ -nickel hydroxide prepared by co-precipitation method are highly dependent on the properties of zinc additive and precipitation pH values. The electrochemical activity is represented by the (101) diffraction line, which increases with increasing pH and the percentage of zinc additive. The  $d_{001}$  value corresponds to interlayer distance  $c_0$  of a brucite-type in hexagonal structure of  $\beta\text{-Ni(OH)}_2$ , which is increases with pH and the percentage of zinc additive. The  $\text{SO}_4^{2-}$ ,  $\text{CO}_3^{2-}$  and  $\text{H}_2\text{O}$  molecules were adsorbed in the samples and the amount of  $\text{SO}_4^{2-}$  ion increases with pH, while  $\text{H}_2\text{O}$  molecule decreases with pH. The variation in the crystal structure and the electrochemical properties of  $\beta\text{-Ni(OH)}_2$  were strongly associated to the amount of adsorbed water as the water content decreased with pH. At a relatively high pH value and zinc additive (6 %), the prepared  $\beta\text{-Ni(OH)}_2$  sample exhibited better electrochemical properties.

## ACKNOWLEDGEMENTS

One of the authors (RCR) thank STIC, Cochin, India for TG-DTG analysis, Indian Institute of Science for providing SEM analysis, BIT, Bangalore, India for FT-IR analysis and Central College, Bangalore, India for XRD analysis.

## REFERENCES

1. P. Oliva, J. Leonardi, J.F. Laurent, C. Delmas, J.J. Braconnier, M. Figlarz, F. Fievet and A. Guibert, *J. Power Sources*, **8**, 229 (1982).
2. B.C. Cornilsen, X.Y. Shan and P.L. Loyselle, *J. Power Sources*, **29**, 453 (1990).
3. R.S. Jayashree, P.V. Kamath and G.N. Subbanna, *J. Electrochem. Soc.*, **147**, 2029 (2000).
4. D. Singh, *J. Electrochem. Soc.*, **145**, 116 (1998).
5. M. Oshitani, T. Takayama, K. Takashima and S. Tsuji, *J. Appl. Electrochem.*, **16**, 403 (1986).
6. H.K. Liu, B. Bright, C.Y. Wang, M. Lindsay and S. Zhong, *J. New Mater. Electrochem. Syst.*, **5**, 50 (2002).
7. K. Watanabe, T. Kikuoka and N. Kumagai, *J. Appl. Electrochem.*, **25**, 219 (1995).
8. Q.S. Song, Ph.D. Dissertation, Tianjin University, China (2000).
9. P.V. Kamath, M. Dixit, L. Indira, A.K. Shukla, V.G. Kumar and N. Munichandraiah, *J. Electrochem. Soc.*, **141**, 2956 (1994).
10. L. Indira, M. Dixit and P.V. Kamath, *J. Power Sources*, **52**, 93 (1994).
11. K. Watanabe and N. Kumagai, *J. Power Sources*, **76**, 167 (1998).
12. P.V. Kamath and G.N. Subbanna, *J. Appl. Electrochem.*, **22**, 478 (1992).
13. L. Demourgues-Guerlou and C. Delmas, *J. Power Sources*, **45**, 281 (1993).
14. C. Delmas, C. Faure and Y. Borthomieu, *Mater. Sci. Eng. B*, **13**, 89 (1992).
15. M. Rajamathi, P.V. Kamath and R. Seshadri, *J. Mater. Chem.*, **10**, 503 (2000).
16. L. Guerlou-Demourgues, C. Denage and C. Delmas, *J. Power Sources*, **52**, 269 (1994).
17. E. Shangguan, Z. Chang, H. Tang, X.-Z. Yuan and H. Wang, *Int. J. Hydrogen Energy*, **35**, 9716 (2010).
18. B. Mani and J.P. Neufville, *J. Electrochem. Soc.*, **135**, 800 (1988).